

Platinum(II) Alkyl Complexes of Chelating DibrIDGEhead Diphosphines
P((CH₂)_n)₃P; Surprisingly Facile *cis/trans* Isomerizations Interconverting
Gyroscope- and Parachute-like Adducts

Yun Zhu,[●] Andreas EhnboM,[●] Tobias Fiedler,^{‡●} Yi Shu, Nattamai Bhuvanesh, Michael
B. Hall,^{*●} and John A. Gladysz^{*●}

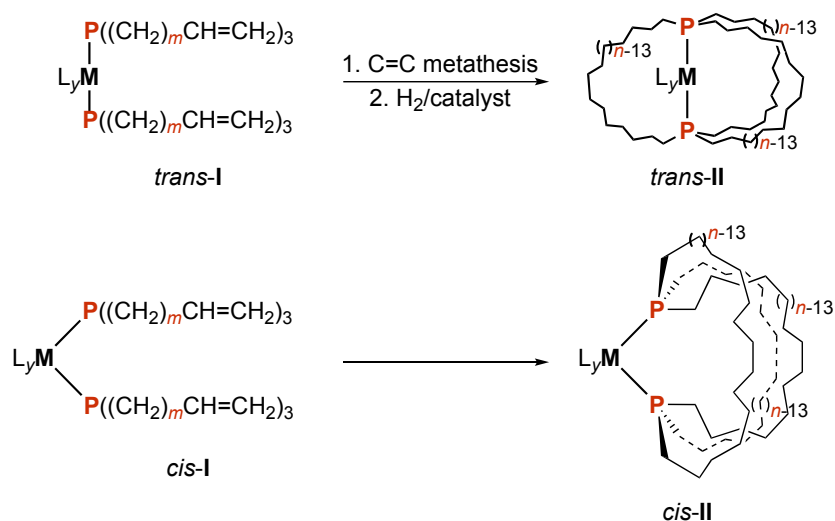
Department of Chemistry, Texas A&M University, PO Box 30012, College Station, Texas
77842-3012, USA

Abstract: Reaction of the gyroscope like dichloride complexes *trans*-Pt(Cl)₂(P(CH₂)_n)₃P (*trans*-**2**; *n* = **c**, 14; **e**, 18; **g**, 22) and MeLi (2 equiv) give the parachute like dimethyl complexes *cis*-Pt(Me)₂(P(CH₂)_n)₃P (*cis*-**3c-g**, 77-91%). Subsequent reactions with HCl (1 equiv) afford *cis*-Pt(Me)(Cl)(P(CH₂)_n)₃P (*cis*-**4c-g**, 83% for **4c**) and after silica gel chromatography or crystallization *trans*-**4c-g** (46-80%) A parallel sequence with *trans*-**2c** and EtLi gives *cis*-Pt(Et)₂(P(CH₂)₁₄)₃P (*cis*-**7c**, 85%) but the subsequent reaction with HCl affords *trans*-Pt(Et)(Cl)(P(CH₂)₁₄)₃P (*trans*-**8c**, 45%) directly. When the previously reported complex *cis*-Pt(Ph)₂(P(CH₂)₁₂)₃P is treated with HCl (1 equiv), *cis*- and *trans*-Pt(Et)(Cl)(P(CH₂)₁₄)₃P (*cis*- and *trans*-**10c**) are isolated in 44% and 29% yields. Reactions of *trans*-**4c** and LiBr or NaI afford the halide complexes *trans*-Pt(Me)(X)(P(CH₂)₁₄)₃P (*trans*-**5c**, *trans*-**6c**) in 88-87% yields. Thermolyses establish strong *trans* preferences for all of the preceding complexes, and the mechanistic implications are analyzed. The crystal structures of *cis*-**3c**, *trans*-**4c**, *trans*-**6c**, and *trans*-**8c** are determined, with the last displaying three independent molecules in the unit cell.

Keywords: platinum, substitution reactions, alkyl complexes, diphosphines, *cis/trans* isomerization. *trans* influence, crystal structures

■ INTRODUCTION

The broad topic of molecular rotors is of importance with respect to several types of molecular machines and devices.¹⁻³ This has driven the synthesis of two classes of metal complexes in our research group. The first would be gyroscope like complexes (*trans-II*, Scheme 1), which can be accessed via ring closing metathesis/hydrogenation sequences involving complexes with *trans* phosphine complexes of the formula $P((CH_2)_mCH=CH_2)_3$ (*trans-I*).³⁻⁷ This results in a cage like dibridgehead diphosphine ligand. Depending upon the length of the methylene segments and the sizes of the ligands, the $P-ML_y-P$ rotators are capable of rotation.

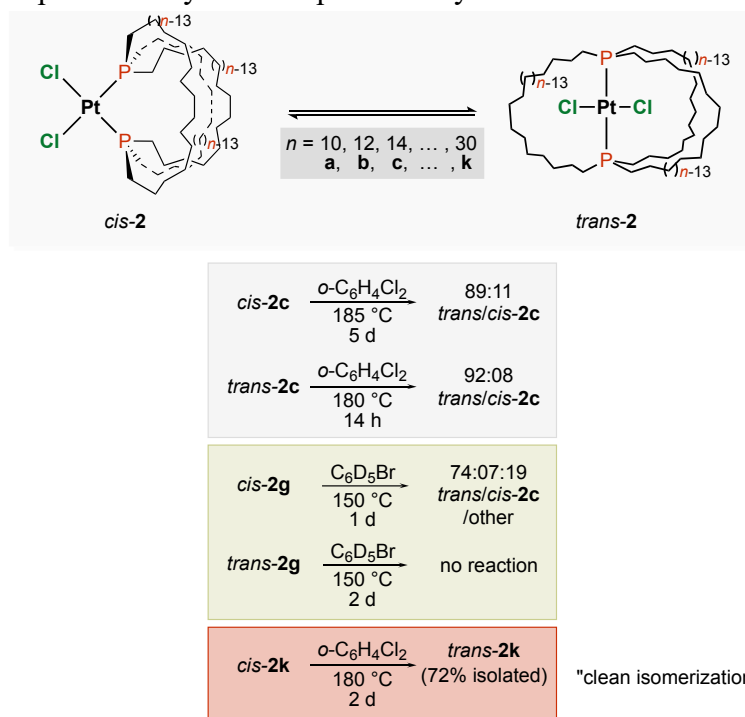


Scheme 1. General syntheses of gyroscope like (*trans-II*) and parachute like (*cis-II*) metal complexes.

When analogous sequences are carried out with certain *cis* complexes (*cis-I*, Scheme 1), the same diphosphine ligands are generated, but now the donor atoms connect *cis* positions.⁸ When generated in square planar or octahedral geometries, one bridge can be visualized as lying in the equatorial plane, another above, and another below. Depending upon the length of the methylene segments and the sizes of the ligands, these bridges are capable of a "jump rope" type dynamic process. This exchanges the positions of the bridges through a series of torsional processes that require rotation about many bonds. When square planar versions of *cis-II* are viewed from an appropriate perspective, there is some resemblance to a parachutist.

In analyzing the dynamic behavior of the gyroscope like complexes *trans-II*, it has always been important to exclude alternative mechanisms for the exchange of ML_y ligands.

Accordingly a *trans/cis* isomerization would open up a new pathway. Specifically, a rapid and thermodynamically uphill initial isomerization to a parachute like *cis-II* complex would be consistent with many observations. Or if the *cis-II* species were more stable, bridge exchange could possibly involve an initial isomerization to *trans-II*. Thus, we have sought to characterize the energetics both experimentally and computationally.



Scheme 2. Previously studied isomerizations.

In two earlier studies, we probed this issue with a series of platinum dichloride complexes.^{4c,8} As shown in Scheme 2, temperatures of ca. 180 °C were required to effect equilibration. The precursor complexes *cis*- and *trans*-(Cl)₂Pt((CH₂)_mCH=CH₂)₃)₂ (*cis*- and *trans*-1) could also be thermally equilibrated.^{4c} Here, in line with literature precedent,^{rf comp?} there was a significant effect of solvent polarity (CH₂Cl₂: appreciable amounts of each isomer; toluene: predominantly *trans*).

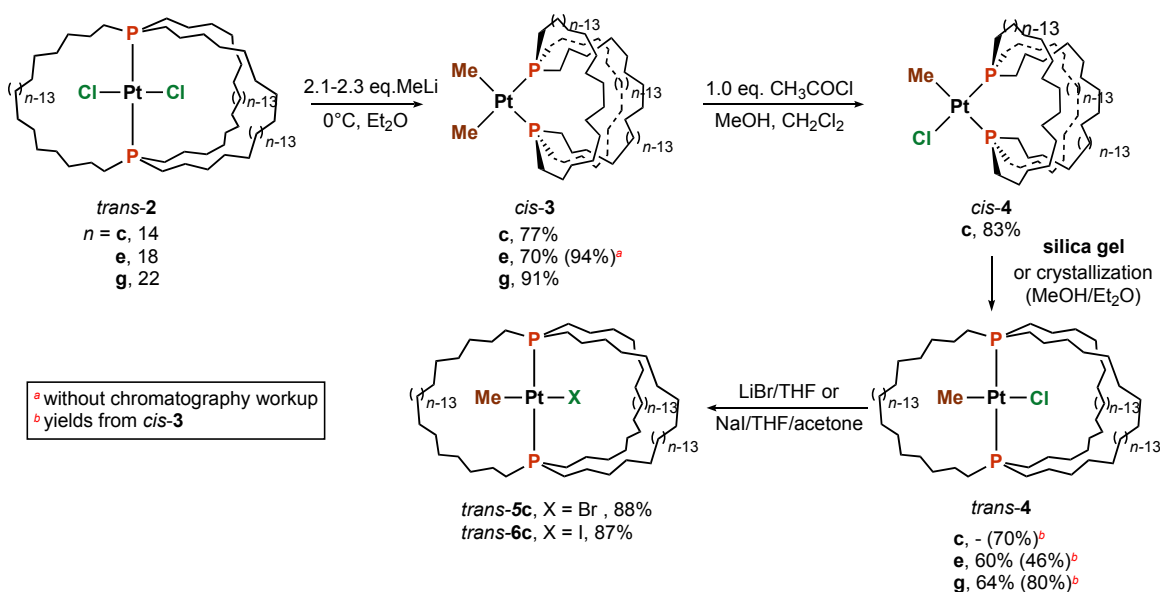
Computationally, as one goes from 13 to 25 membered macrocycles (or **2a** to **2g**) methylene groups per bridge), the gyroscope like complexes *trans-2* range from 5.1 to 9.2 kcal/mol more stable.⁸ However, the energy differences do not vary monotonically. Rather, there is an even/odd alternation with respect to *n*/2 (odd, -9.2 to -8.5 kcal/mol; even, -5.8 to -5.1

kcal/mol).

In this paper, we report the surprising observation that low energy pathways exist for the interconversion of the preceding types of complexes when the two chloride ligands are replaced by alkyl ligands. This unexpected result also prompted us to attempt thermal equilibrations of previously prepared phenyl substituted complexes.^{4a,9}

■ RESULTS

1. Syntheses and NMR characterization. The gyroscope like platinum dichloride complexes *trans*-Pt(Cl)₂(P(CH₂)_n)₃P (*trans*-**2**; *n* = **c**, 14; **d**, 16; **e**, 18) were prepared as previously described.^{4a} Diethyl ether solutions of MeLi were added (2.1 equiv). After 12 h at 0 °C (for **2c**, the same result was obtained at room temperature), chromatographic workups (neutral alumina) gave the new dimethyl complexes *cis*-Pt(Me)₂(P(CH₂)_n)₃P (*cis*-**3c,e,g**) in 77-91% yields as white **air stable** solids. These and all other new complexes below were characterized by microanalyses and NMR (¹H, ¹³C, ³¹P). The *cis* coordination geometry was evidenced by the diagnostic ¹J_{Pt} values (1853-1886 Hz)¹² The ¹³C{¹H} NMR spectra showed doublets of doublets for the methyl groups (*cis*-**3c**: ²J_{CP(trans)} = 101.7 Hz, ²J_{CP(cis)} = 9.9 Hz). The ¹H NMR spectra also showed doublets of doublets (*cis*-**3c**: ³J_{HP(trans)} = 7.1 Hz, ³J_{HP(cis)} = 6.1 Hz), and platinum satellites were usually visible (*cis*-**3c**: ²J_{HPt(195)} = 66 Hz).

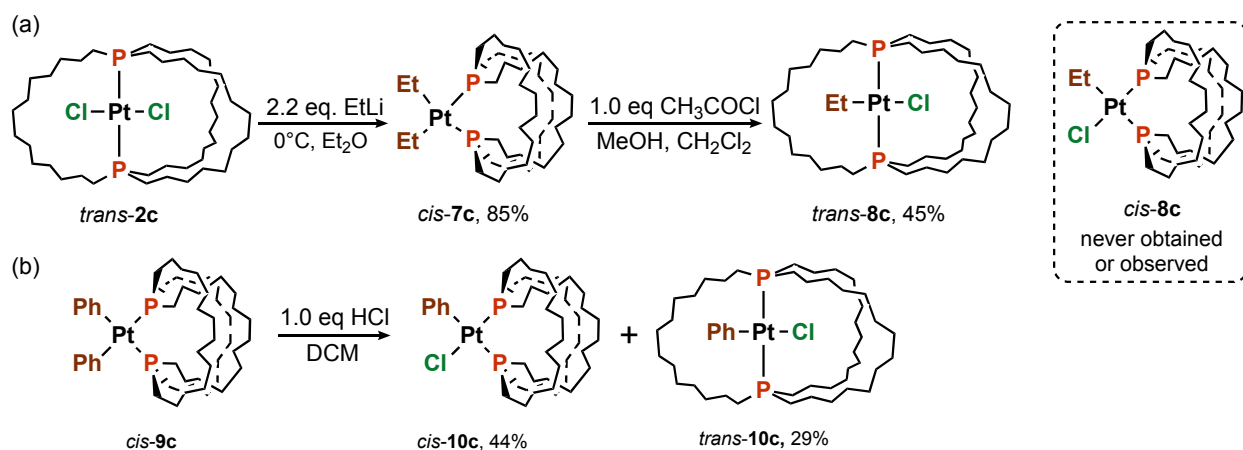


Scheme 3. Substitution and isomerization reactions involving methyl ligands.

A reaction of *trans-2c* and 1.1 equiv of MeLi was similarly conducted. A $^{31}\text{P}\{^1\text{H}\}$ NMR spectrum of the crude reaction mixture showed 40-50% conversion to the dimethyl complex *cis-3c*. The only other signal detected was that of the starting material *trans-2c* (no *trans-3c* or *cis-2c* were detected).

Next, CH_2Cl_2 solutions of *cis-3c,e,g* were treated with 1.0? equiv of HCl (generated in situ from 1.0? equiv of acetyl chloride and excess methanol). Chromatographic workups (neutral alumina) gave monomethyl monochloride complexes *cis-4c,e,g* in 83-XX% yields. The stereochemistry was evidenced by coupling phenomena involving the ^1H and ^{13}C NMR methyl signals analogous to those obtained for *cis-3c,e,g*. Also, the $^{31}\text{P}\{^1\text{H}\}$ NMR spectra now showed two signals, one for the phosphorus atom *trans* to the methyl ligand and another for the atom *trans* to the chloride ligand. Now the $^2J_{\text{PPt}(195)}$ values differed significantly (1765-1XXX vs. 4278-4XXX Hz).

When *cis-4c* was passed through silica gel, or crystallized from diethyl ether/MeOH, *trans-4c* was obtained. Now the methyl ^1H and ^{13}C NMR signals were triplets, reflecting coupling to two equivalent phosphorus atoms. A single ^{31}P signal was observed, now with a $^1J_{\text{PPt}(195)}$ value of 2824 Hz.



Scheme 4. Substitution and isomerization reactions involving ethyl and phenyl ligands.

As shown in Scheme 4(a), a parallel sequence was carried out with *trans-2c* and EtLi in place of MeLi. Accordingly, the corresponding diethyl complex *cis-7c* was isolated in 85% yield after workup. Although the methyl group is now further from the platinum, the ^1H NMR

spectrum again showed a dd, indicative of coupling to two phosphorus atoms (asked Yun why not further coupling to CH₂). The ³¹P{¹H} NMR spectrum exhibited a single signal with a ¹J_{PPt(195)} value of 1746 Hz.

Next, *cis-7c* was treated with HCl analogously to the reaction of the dimethyl complex *cis-3c*. Now, the same workup (neutral alumina) delivered *trans-8c* in 45% yield. This was clearly evidenced by the single ³¹P{¹H} NMR signal (¹J_{PPt(195)} = 3002 Hz).

2. Dynamic and solid state properties. Although it was not the purpose of the study to characterize the dynamic properties of the title molecules, some useful information can be gleaned *en passant*. With square planar gyroscope like complexes, no conformation exists in which the three (CH₂)_n segments can be exchanged by a symmetry operation (two may be). Thus, there should be more than one set of (CH₂)_n ¹³C NMR signals. However, *trans-4c* and *trans-8c* exhibit only one. This requires (in the absence of special mechanisms, such as ligand dissociation or others considered below), rapid Cl-Pt-R rotation on the NMR time scale. We have noted other methyl substituted rotors that can rapidly pass through macrocycles that contain fourteen methylene groups ((CH₂)₁₄ bridges).^{5c,7} However, this is the first case in which a similar time scale has been verified for an ethyl group.

As noted above, one of the (CH₂)_n segments in the parachute like complexes can be viewed as laying in the metal coordination plane. All of the *cis* complexes noted above exhibit two sets of signals in approximately a 2:1 area ratio (whoa, *cis* Me-Pt-Cl seems to exhibit three).

Due to the many steric and dynamic features of interest in the preceding classes of molecules, we have endeavored to acquire structural data whenever possible. Accordingly, single crystals of *cis-3c*, *trans-4c*, and *trans-8c* could be obtained, and the X-ray structures were determined as outlined in Table 1 and the experimental section. Thermal ellipsoid plots are depicted in Figures 1-3?. Key metrical parameters are listed in Table 2.

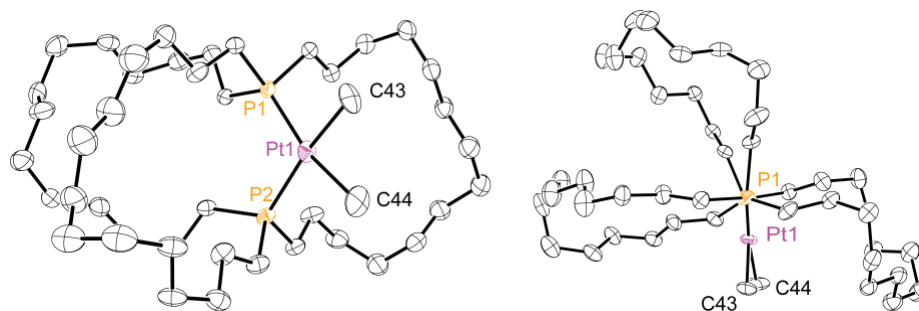


Figure 1. Thermal ellipsoid plots of the molecular structure of *cis-3c* (50% probability level).

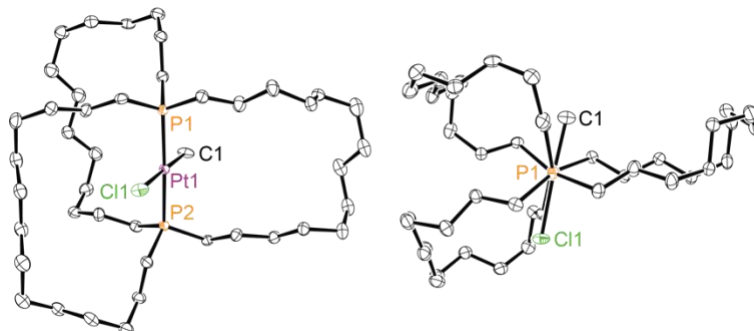


Figure 2. ORTEPS from Tobias' X-ray writeup but best if they are from Yun's structure and not Yi's Thermal ellipsoid plots of the dominant conformation of *trans-4c* in the crystal lattice (50% probability level).

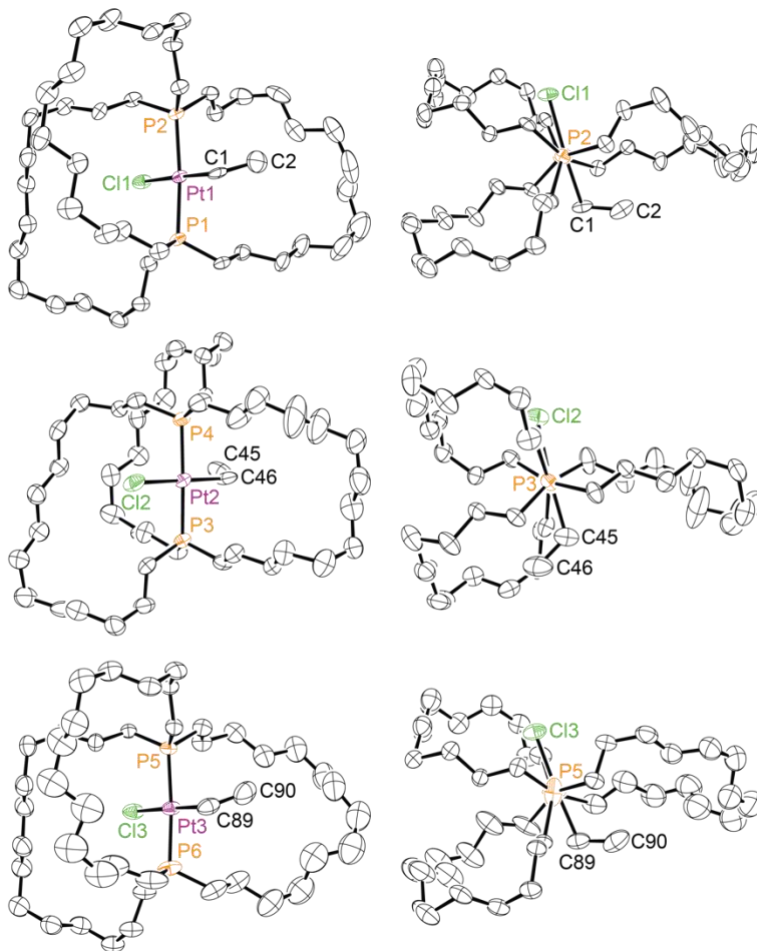


Figure 3. ORTEPS from Tobias' X-ray writeup Thermal ellipsoid plots of the three independent molecules of *trans*-**8c** in the crystal lattice (50% probability level).

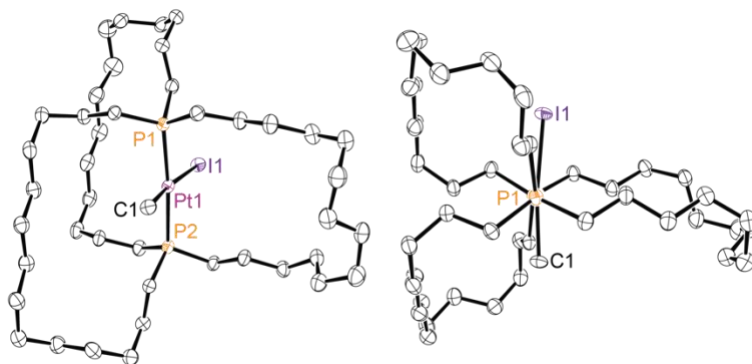


Figure 4. ORTEPS from Tobias' X-ray writeup Thermal ellipsoid plots of the dominant conformation of the IODIDE complex corresponding to *trans*-**6c** (50% probability level)

The other metrical parameters associated with the new complexes were routine, resembling those found in related species earlier. For example, ...

3. Computational data. In order to better interpret the relative stabilities of cis/trans

isomers described above, DFT calculations, including dispersion corrections, were carried out as reported earlier.⁸ This was followed by molecular dynamics annealing simulations to maximize the likelihood of correctly identifying the lowest energy conformer. This output was further optimized by additional DFT calculations. As shown in Figure s9 (SI), the dispersion corrections gave structures that more closely modeled those in the crystal structures.

Recycled text: The relative gas phase stabilities of the parachute and gyroscope like complexes *cis-X* and *trans-X* are illustrated as a function of macrocycle size in Figure 5. As one goes from thirteen to twenty five membered macrocycles (or ten (**a**) to twenty-two (**g**) methylene groups per bridge), the gyroscope like complexes range from 5.1 to 9.2 kcal/mol more stable, consistent with the trends established in haloarenes in Figures ???. However, the energy differences do not vary monotonically. Rather, there is an "even/odd" alternation with respect to $n/2$ (odd, -9.2 to -8.5 kcal/mol; even, -5.8 to -5.1 kcal/mol). No attempt has been made to elucidate a basis for this phenomenon. However, it may be coupled to conformational features of the macrocycles.

Figure 5. Relative energies (kcal/mol) of isomeric platinum complexes as computed by DFT and molecular dynamics (gas phase).

4. Thermolyses.

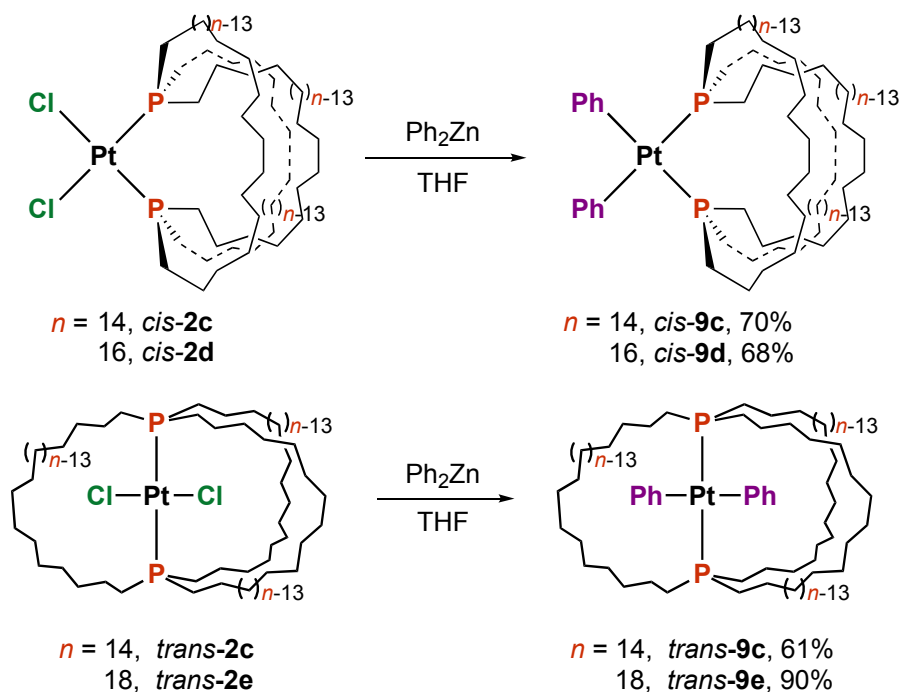
Table 1. Summary of thermal equilibration data

X	X'	Solvent	Temperature (°C)	Time (h)	<i>cis/trans</i> ratio ^a
		toluene-d ₈	80	10	>99:1
Me	Me	C ₆ D ₅ Br	140	6	<1:99 ^b
		<i>o</i> -C ₆ H ₄ Cl ₂	140	12	<1:99 ^b
Me	Cl	toluene-d ₈	80	10	86:14 ^c
		C ₆ D ₅ Br	110	7	<1:99
		<i>o</i> -C ₆ H ₄ Cl ₂	100	3	<1:99
		<i>o</i> -C ₆ H ₄ Cl ₂	140	0.5	<1:99
Ph	Ph	toluene-d ₈	80	10	>99:1
		C ₆ H ₄ Cl ₂	140	7	1:90:(9) ^d
Ph	Cl	<i>o</i> -C ₆ H ₄ Cl ₂	100	6	1:99
		<i>o</i> -C ₆ H ₄ Cl ₂	140	0.5	1:99

^aDetermined via ³¹P{¹H} NMR. ^bIn the *trans* species, one of the methyl groups was replaced by halogen atom from the solvent. ^cNot the final equilibrium ratio. ^dThe percentage in the parenthesis indicated an unidentified species.

■ DISCUSSION

blah blah blah



Scheme 5. Some previously studied substitution reactions that fit the rigorous textbook definition of stereospecific.

In square planar gyroscope like complexes, the transition states for rotation would normally involve passage of one ligand of a rotator through a single macrocycle, as shown in **II**.

In summary, this study has expanded the toolbox of substitution reactions applicable to gyroscope like complexes, and provided additional data and insight regarding their dynamic properties. Future efforts will extend these themes to additional coordination geometries,^{3g} including syntheses of other types of complexes with dipolar rotators, and minimization of the rotational barriers therein.

■ Experimental Section

General. Reactions were conducted under nitrogen atmospheres unless noted. NMR spectra were recorded on standard 500 MHz FT spectrometers and referenced as follows (σ , ppm): ^1H , residual internal CH_2Cl_2 (5.32) or $\text{THF-}d_7$ (1.73); $^{13}\text{C}\{^1\text{H}\}$, internal CD_2Cl_2 (53.8) or $\text{THF-}d_8$ (25.2); $^{31}\text{P}\{^1\text{H}\}$, internal 85% H_3PO_4 capillary (0.0). Other instruments employed have been detailed in earlier papers.⁴

Chemicals were treated as follows: CH_2Cl_2 , distilled from CaH_2 (for reactions) or simple distillation (chromatography); hexanes, ether, and methanol, simple distillation; CDCl_3 , celite (EMD), and neutral alumina (Macherey-Nagel), used as received. Complex *trans-2c* was synthesized by literature procedures. need now list of chemicals like in other papers

NMR spectra were recorded on Bruker 500 MHz spectrometer at ambient probe temperatures and referenced as follows: ^1H : residual internal CHCl_3 (δ , 7.26 ppm), $\text{C}_6\text{H}_5\text{Br}$ (δ , 7.40 ppm for the most down field signal), ^{13}C : internal CDCl_3 (δ , 77.16 ppm), ^{31}P : external H_3PO_4 (δ , 0.00 ppm). Mass spectra data were recorded on a Micromass Zabspec instrument. Melting points were determined on an Electrothermal IA 9100 apparatus or a Stanford Research Systems (SRS) MPA100 (Opti-Melt) automated device. Microanalyses were conducted in house (Carlo Erba EA1110 instrument) or by Atlantic Microlab.

***cis-Pt(Me)₂(P((CH₂)₁₄)₃P)* (*cis-3c*).** A Schlenk flask was charged with *trans-PtCl₂(P((CH₂)₁₄)₃P)* (*trans-2c*;^{4a} 0.2242 g, 0.2445 mmol) and diethyl ether (12 mL). Then MeLi (1.6 M in diethyl ether, 0.330 mL, 0.528 mmol) was added at room temperature with stirring. After 12 h, the mixture was exposed to air. After 1 h, the sample was filtered through celite, which was washed with diethyl ether (10-20 mL). The solvent was removed from the filtrate by rotary evaporation. The residue was chromatographed on neutral alumina (1:0.005 v./v hexanes/ Et_3N). The solvent was removed from the product containing fractions (TLC monitoring) by rotary evaporation. The oil was kept at 4 °C, and after 2 d gave *cis-3c* a white solid (0.1645 g, 0.1877 mmol, 77%), mp (capillary) 80-83 °C. Anal. Calcd. for $\text{C}_{44}\text{H}_{90}\text{P}_2\text{Pt}$: C, 60.31; H, 10.35. Found: C, 60.59; H, 10.55.

NMR (CDCl₃, δ /ppm):⁴⁵ ¹H (500 MHz) 1.90-1.78 (br m, 4H, PCH₂), 1.72-1.50 (br m, 12H, CH₂), 1.50-1.21 (br m, CH₂), 0.30 (dd, 6H, ³J_{HP(trans)} = 7.1 Hz, ³J_{HP(cis)} = 6.1 Hz, ²J_{HPt(195)} = 66 Hz,⁴⁶ PtCH₃); ¹³C{¹H} (126 MHz) 31.1 (virtual t,⁴⁷ J_{CP} = 4.2 Hz, CH₂), 30.5 (virtual t,⁴⁷ J_{CP} = 6.6 Hz, CH₂), 28.3 (s, CH₂), 27.52 (s, CH₂), 27.46 (s, CH₂), 27.2 (s, CH₂), 26.9 (s, CH₂), 26.46 (s, CH₂), 26.35 (s, CH₂), 24.8 (virtual t,⁴⁷ J_{CP} = 10.5 Hz, CH₂), 23.3 (virtual t,⁴⁷ J_{CP} = 15.1 Hz, CH₂), 2.75 (dd, ²J_{CP(trans)} = 101.7 Hz, ²J_{CP(cis)} = 9.9 Hz, PtCH₃); ³¹P{¹H} (202 MHz) 6.90 (s, ¹J_{PPt(195)} = 1886 Hz).⁴⁶ MS:⁴⁸ 875.6 ([M]⁺, 19%), 860.6 ([M-CH₃]⁺, 100%).

cis-Pt(Me)₂(P((CH₂)₁₈)₃P) (cis-3e). A Schlenk flask was charged with *trans*-PtCl₂(P((CH₂)₁₈)₃P) (*trans*-**2e**;^{4a} 0.1239 g, 0.1142 mmol) and diethyl ether (20 mL). Then MeLi (1.6 M in diethyl ether, 0.160 mL, 0.256 mmol) was added at room temperature with stirring. After 12 h, the mixture was exposed to air. After 1 h, the sample was filtered through celite, which was washed with diethyl ether (10-20 mL). The solvent was removed from the filtrate by rotary evaporation. The residue was chromatographed on neutral alumina with (1:0.005 v/v hexanes/Et₃N). The solvent was removed from the product containing fractions (TLC monitoring) by rotary evaporation to give *cis*-**3e** as a colorless oil (0.0838 g, 0.0802 mmol, 70%).

NMR (CDCl₃, δ /ppm):⁴⁵ ¹H (500 MHz) 1.77-1.64 (br m, 12H, PCH₂), 1.48-1.39 (br m, 12H, CH₂), 1.39-1.33 (br m, 12H, CH₂), 1.33-1.18 (br m, 72H, remaining CH₂), 0.33 (dd, 6H, ³J_{HP(trans)} = 6.7 Hz, ³J_{HP(cis)} = 5.7 Hz, ²J_{HPt(195)} = 65 Hz,⁴⁶ PtCH₃); ¹³C{¹H} (126 MHz) 31.5 (virtual t,⁴⁷ J_{CP} = 5.9 Hz, CH₂), 29.3 (s, CH₂), 29.0 (s, CH₂), 28.5 (s, CH₂), 27.9 (s, CH₂), 27.6 (s, CH₂), 27.2 (s, CH₂), 24.7 (virtual t,⁴⁷ J_{CP} = 9.1 Hz, CH₂), 2.61 (dd, ²J_{CP(trans)} = 101.1 Hz, ²J_{CP(cis)} = 10.0 Hz, PtCH₃); ³¹P{¹H} (202 MHz) 4.51 (s, ¹J_{PPt(195)} = 1860 Hz).⁴⁶

cis-Pt(Me)₂(P((CH₂)₂₂)₃P) (cis-3g). A Schlenk flask was charged with *trans*-PtCl₂(P((CH₂)₂₂)₃P) (*trans*-**2g**;^{4c} 0.1469 g, 0.1172 mmol) and diethyl ether (20 mL). Then MeLi (1.6 M in diethyl ether, 0.170 mL, 0.272 mmol) was added at room temperature with stirring. After 12 h, the mixture was exposed to air. After 1 h, the sample was filtered through celite, which was washed with diethyl ether (10-20 mL). The solvent was removed from the filtrate by rotary

evaporation. The residue was dissolved in benzene and the solvent was removed by freeze drying to give *cis*-**3g** as a white powder (0.1294g, 0.1067 mmol, 91%), mp (capillary) 55-60 °C. Anal. Calcd. for C₆₈H₁₃₈P₂Pt: C, 67.34; H, 11.47. Found: C, 67.61; H, 11.64.

NMR (CDCl₃, δ/ppm):⁴⁵ ¹H (500 MHz) 1.90-1.79 (br m, 12H, PCH₂), 1.70-1.58 (br m, 12H, CH₂), 1.49-1.42 (br m, 12H, CH₂) 1.42-1.32 (br m, 96H, remaining CH₂), 1.08 (dd, 6H, ³J_{HP(trans)} = 7.3 Hz, ³J_{HP(cis)} = 6.1 Hz, ²J_{HPt(195)} = 66 Hz, ⁴⁶ PtCH₃); ¹³C{¹H} (126 MHz) 31.98 (virtual t, ⁴⁷ J_{CP} = 5.8 Hz, CH₂), 29.98 (s, CH₂), 29.97 (s, CH₂), 29.85 (s, CH₂), 29.50 (s, CH₂), 28.45 (s, CH₂), 28.17 (s, CH₂), 27.85 (s, PCH₂CH₂), 25.21 (virtual t, ⁴⁷ J_{CP} = 9.3 Hz, CH₂), 3.86 (dd, ²J_{CP(trans)} = 101.7 Hz, ²J_{CP(cis)} = 10.0 Hz, PtCH₃); ³¹P{¹H} (202 MHz) 4.56 (s, ¹J_{PPt(195)} = 1853 Hz).⁴⁶

cis-Pt(Cl)(Me)(P((CH₂)₁₄)₃P) (*cis*-**4c**). Under air, a round bottom flask was charged with *cis*-**3c** (0.4007 g, 0.4573 mmol), dichloromethane (10 mL), and methanol (1.0 mL). Then CH₃COCl (0.0344 mL, 0.4865 mmol) was added with stirring. After 30 min, the solvent was removed by rotary evaporation. The white solid was chromatographed on neutral alumina (25:1:0.2 v/v/v hexanes/ethyl acetate/Et₃N). The solvent was removed from the product containing fractions (TLC monitoring) by rotary evaporation. This gave *cis*-**4c** as a white solid (0.3610 g, 0.4026 mmol, 83%), mp (capillary) 122-127 °C. Anal. Calcd. for C₄₃H₈₇ClP₂Pt: C, 57.60; H, 9.78. Found: C, 57.80; H, 10.00.

NMR (CDCl₃, δ/ppm):⁴⁵ ¹H (500 MHz) 2.42-2.33 (br m, 2H, PCH₂), 1.92-1.83 (br m, 2H, CH₂), 1.82-1.68 (br m, 6H, CH₂), 1.68-1.53 (br m, 6H, CH₂), 1.50-1.21 (br m, 68H, remaining CH₂), 0.58 (dd, 3H, ³J_{HP(trans)} = 7.0 Hz, ³J_{HP(cis)} = 4.0 Hz, ²J_{HPt(195)} = 50 Hz, ⁴⁶ PtCH₃); ¹³C{¹H} (126 MHz) 30.9 (virtual t, ⁴⁷ J_{CP} = 10.5 Hz, CH₂), 30.6 (s, CH₂), 30.5 (s, CH₂), 30.4 (s, CH₂), 30.2 (s, CH₂), 28.5 (s, CH₂), 28.3 (s, CH₂), 27.7 (s, CH₂), 27.4 (s, CH₂), 27.29 (s, CH₂), 27.26 (s, CH₂), 27.1 (s, CH₂), 27.0 (s, CH₂), 26.94 (s, CH₂), 26.90 (s, CH₂), 26.88 (s, CH₂), 26.83 (s, CH₂), 26.33 (s, CH₂), 26.26 (s, CH₂), 26.23 (s, CH₂), 25.0 (virtual t, ⁴⁷ J_{CP} = 4.0 Hz, CH₂), 23.9 (s, CH₂), 23.6 (s, CH₂), 23.5 (s, CH₂), 22.8 (virtual t, ⁴⁷ J_{CP} = 7.3 Hz, CH₂), 4.48 (dd, ²J_{CP(trans)} = 93.1 Hz, ²J_{CP(cis)} = 8.0 Hz, PtCH₃); ³¹P{¹H} (202 MHz) 11.6 (d,

$^2J_{PP} = 12.1$ Hz, $^1J_{PPt(195)} = 1765$ Hz,⁴⁶ *trans* to CH₃), 5.0 (d, $^2J_{PP} = 12.1$ Hz, $^1J_{PPt(195)} = 4278$ Hz,⁴⁶ *cis* to CH₃).

***trans*-Pt(Cl)(Me)(P((CH₂)₁₄)₃P) (*trans*-4c).** Under air, a round bottom flask was charged with *cis*-3c (0.245g, 0.0273 mmol), silica gel (0.2577g), and dichloromethane (2.5 mL). The mixture was stirred at room temperature. After 12 h, the sample was filtered and the silica gel further washed with dichloromethane (25 mL). The solvent was removed from the filtrate by rotary evaporation to yield a colorless oil, which solidified after 4 h to give *trans*-4c (0.0174 g, 0.0192 mmol, 70%) as a white solid. mp (capillary) 123-127 °C. Anal. Calcd. for C₄₃H₈₇ClP₂Pt: C, 57.60; H, 9.78. Found: C, 57.85; H, 10.05.

Crystallization: Under air, a vial was charged with a solution of *cis*-4c in diethyl ether. Then ethanol was slowly added. The mixture was shaken after each drop to redissolve the white precipitate formed. When the precipitate persisted, diethyl ether was added to generate a homogeneous solution. The solution was kept in a vial at 4 °C. After 2 d, a colorless prism of *trans*-4c formed.

NMR (CDCl₃, δ/ppm):⁴⁵ ¹H (500 MHz) 1.85-1.73 (br m, 12H, PCH₂), 1.65-1.55 (br m, 12H, PCH₂CH₂), 1.48-1.38 (br m, 12H, PCH₂CH₂CH₂), 1.38-1.23 (br m, 48H, remaining CH₂), 0.31 (t, 3H, $^3J_{HP(trans)} = 6.2$ Hz, $^2J_{HPt(195)} = 83$ Hz,⁴⁶ CH₃); ¹³C{¹H} (126 MHz) 30.2 (virtual t,⁴⁷ $J_{CP} = 6.7$ Hz), 28.3 (s, CH₂), 27.4 (s, CH₂), 27.3 (s, CH₂), 27.0 (s, CH₂), 23.5 (s, CH₂), 22.0 (virtual t,⁴⁷ $J_{CP} = 15.7$ Hz, CH₂), -23.6 (virtual t,⁴⁷ $J_{CP} = 6.4$ Hz, PtCH₃); ³¹P{¹H} (202 MHz) 6.6 (s, $^1J_{PPt(195)} = 2824$ Hz).⁴⁶

***cis*-Pt(Cl)(Me)(P((CH₂)₁₈)₃P) (*cis*-4e) and *trans*-Pt(Cl)(Me)(P((CH₂)₁₈)₃P) (*trans*-4e).**
A. Under air, a round bottom flask was charged with *cis*-3e (0.0838 g, 0.0802 mmol), dichloromethane (8 mL), and methanol (0.4 mL). Then a HCl (2.0 M in Et₂O, 0.040 mL, 0.080 mmol) was added with stirring. After 30 min, the solvent was removed by rotary evaporation. The white solid was chromatographed on neutral alumina (first 3:1:0.02 v/v/v hexanes/dichloromethane/Et₃N and then 25:1:0.2 v/v/v hexanes/ethyl acetate/Et₃N). The solvent was removed from the product containing fractions (TLC monitoring) by rotary evaporation.

This gave *trans*-**4e** (0.0389 g, 0.0365 mmol, 46%), with subsequent fractions affording *trans*-**4e**/*cis*-**4e** mixtures.

B. A vial was charged with a *trans*-**4e**/*cis*-**4e** mixture (ca. 1:2 by ^{31}P NMR; 0.0274 g, 0.0257 mmol) obtained from a different run, silica gel (1.2375 g) and dichloromethane (10 mL). The mixture was stirred at room temperature. After 12 h, the sample was filtered and the silica gel further washed with dichloromethane (40 mL). The solvent was removed from the filtrate to give *trans*-**4e** (0.0165 g, 0.0155 mmol, 60%) as a beige oil.

Data for *cis*-**4e**: NMR (CDCl_3 , δ/ppm): $^{31}\text{P}\{^1\text{H}\}$ (202 MHz) 10.3 (d, $^2J_{\text{PP}} = 12.1\text{Hz}$, *trans* to CH_3), 3.56 (d, $^2J_{\text{PP}} = 12.1\text{Hz}$, *cis* to CH_3).

Data for *trans*-**4e**: NMR (CDCl_3 , δ/ppm):⁴⁵ ^1H (500 MHz) 1.88-1.75 (br m, 12H, PCH_2), 1.65-1.50 (br m, 12H, PCH_2CH_2), 1.46-1.38 (br m, 12H, $\text{PCH}_2\text{CH}_2\text{CH}_2$), 1.38-1.23 (br m, 72H, remaining CH_2), 0.31 (t, 3H, $^3J_{\text{HP}(\text{trans})} = 6.2\text{ Hz}$, $^2J_{\text{HPt}(195)} = 83\text{ Hz}$,⁴⁶ CH_3); $^{13}\text{C}\{^1\text{H}\}$ (126 MHz) 30.82 (virtual t,⁴⁷ $J_{\text{CP}} = 6.4\text{ Hz}$), 28.64 (s, CH_2), 28.48 (s, CH_2), 28.47 (s, CH_2), 28.35 (s, CH_2), 28.04 (s, CH_2), 27.78 (s, CH_2), 23.89 (s, CH_2), 21.49 (virtual t,⁴⁷ $J_{\text{CP}} = 15.9\text{ Hz}$, CH_2), -23.41 (virtual t,⁴⁷ $J_{\text{CP}} = 6.46\text{ Hz}$, PtCH_3); $^{31}\text{P}\{^1\text{H}\}$ (202 MHz) 8.8 (s, $^1J_{\text{PPt}(195)} = 2824\text{ Hz}$).⁴⁶

***cis*-Pt(Cl)(Me)(P((CH₂)₂₂)₃P) (*cis*-**4g**)**

***trans*-Pt(Cl)(Me)(P((CH₂)₂₂)₃P) (*trans*-**4g**).** **A.** Under air, a vial was charged with *cis*-**3g** (0.146g, 0.0120 mmol), silica gel (0.2572g) and dichloromethane (2.5 mL). The mixture was stirred at room temperature. After 12 h, the sample was filtered and the silica gel further washed with dichloromethane (25 mL). The solvent was removed from the filtrate by rotary evaporation to give *trans*-**4c** (0.0118 g, 0.0096 mmol, 80%) as a colorless oil.

B. A vial was charged with a *trans*-**4g**/*cis*-**4g** mixture (1:18 by ^{31}P NMR; 0.0350 g, 0.0284 mmol), obtained from a different run, silica gel (0.9325 g) and dichloromethane (10 mL). The mixture was stirred at room temperature. After 12 h, the sample was filtered and the silica gel further washed with dichloromethane (40 mL). The solvent was removed from the filtrate to give *trans*-**4e** (0.0224 g, 0.0182 mmol, 64%) as a beige oil.

NMR (CDCl₃, δ/ppm):⁴⁵ ¹H (500 MHz) 1.89-1.74 (br m, 12H, PCH₂),⁴⁵ 1.62-1.47 (br m, 12H, PCH₂CH₂), 1.45-1.35 (br m, 12H, PCH₂CH₂CH₂), 1.35-1.18 (br m, 96H, remaining CH₂), 0.31 (t, 3H, ³J_{HP(trans)} = 6.2 Hz, ²J_{HPt(195)} = 84 Hz,⁴⁶ CH₃); ¹³C{¹H} (126 MHz) 31.27 (virtual t,⁴⁷ J_{CP} = 6.35 Hz), 29.42 (s, CH₂), 29.24 (s, CH₂), 29.18 (s, CH₂), 29.08 (s, CH₂), 28.89 (s, CH₂), 28.57 (s, CH₂), 28.52 (s, CH₂), 28.30 (s, CH₂), 24.13 (s, CH₂), 21.54 (virtual t,⁴⁷ J_{CP} = 15.8 Hz, CH₂), -23.12 (virtual t,⁴⁷ J_{CP} = 6.6 Hz, PtCH₃); ³¹P{¹H} (202 MHz) 8.3 (s, ¹J_{PPt(195)} = 2796 Hz).⁴⁶

***trans*-Pt(Br)(Me)(P((CH₂)₁₄)₃P) (*trans*-5c)** A Schlenk flask was charged with *trans*-4c (0.0981 g, 0.1094 mmol), LiBr (0.0488 g, 0.562 mmol) and THF (10 mL). The mixture was stirred at room temperature. After 12 h, the sample was concentrated and chromatographed on silica gel (3:2 v/v hexanes/dichloromethane). The solvent was removed from the product containing fractions (TLC monitoring) to give *trans*-5c as a colorless oil, which solidified after 1 h (0.0903 g, 0.0960 mmol, 88%), mp (capillary) 110-119 °C. Anal. Calcd. for C₄₃H₈₇BrP₂Pt: C, 54.88; H, 9.32. Found: C, 55.74; H, 9.51.

NMR (CDCl₃, δ/ppm):⁴⁵ ¹H (500 MHz) 1.95-1.73 (br m, 12H, PCH₂), 1.66-1.52 (br m, 12H, PCH₂CH₂), 1.48-1.37 (br m, 12H, PCH₂CH₂CH₂), 1.37-1.20 (br m, 48H, remaining CH₂), 0.39 (t, 3H, ³J_{HP} = 6.1 Hz, ²J_{HPt(195)} = 82 Hz,⁴⁶ CH₃); ¹³C{¹H} (126 MHz) 30.1 (virtual t,⁴⁷ J_{CP} = 6.8 Hz), 28.3 (s, CH₂), 27.4 (s, CH₂), 27.3 (s, CH₂), 26.9 (s, CH₂), 23.5 (s, CH₂), 22.5 (virtual t,⁴⁷ J_{CP} = 16.0 Hz, CH₂), -20.2 (virtual t,⁴⁷ J_{CP} = 6.4 Hz, PtCH₃); ³¹P{¹H} (202 MHz) 8.5 (s, ¹J_{PPt(195)} = 2804 Hz).⁴⁶

***trans*-Pt(I)(Me)(P((CH₂)₁₄)₃P) (*trans*-6c)** Under air, a vial was charged with *trans*-4c (0.0599 g, 0.0668 mmol), NaI (0.0557 g, 0.372 mmol), THF (4 mL) and acetone (4 mL). The mixture was stirred at room temperature for 2 d. The sample was concentrated and chromatographed on silica gel (hexanes, then dichloromethane). The solvent was removed from two sets of product fractions (TLC monitoring) to give *trans*-PtI₂(P((CH₂)₁₄)₃P) (0.0077 g, 0.007 mmol, 10%)^{4a} and *trans*-6c (0.0577 g, 0.0584 mmol, 87%) as yellow waxy oils that solidified after 2-4 h, mp (capillary, *trans*-6c) 114-118 °C. Anal. Calcd. for C₄₃H₈₇I₂P₂Pt: C,

52.27; H, 8.88. Found: C, 51.99; H, 8.91.

NMR (CDCl₃, δ /ppm):⁴⁵ ¹H (500 MHz) 2.01-1.88 (br m, 12H, PCH₂), 1.61-1.50 (br m, 12H, PCH₂CH₂), 1.47-1.38 (br m, 12H, PCH₂CH₂CH₂), 1.37-1.19 (br m, 48H, remaining CH₂), 0.48 (t, 3H, ³J_{HP} = 6.2 Hz, ²J_{HPt(195)}} = 81.5 Hz,⁴⁶ CH₃); ¹³C{¹H} (126 MHz) 30.1 (virtual t,⁴⁷ J_{CP} = 6.6 Hz), 28.2 (s, CH₂), 27.4 (s, CH₂), 27.3 (s, CH₂), 26.9 (s, CH₂), 23.9 (virtual t,⁴⁷ J_{CP} = 15.7 Hz, CH₂), 23.5 (s, CH₂), -14.8 (virtual t,⁴⁷ J_{CP} = 6.2 Hz, PtCH₃); ³¹P{¹H} (202 MHz) 5.4 (s, ¹J_{Pt(195)}} = 2767 Hz).⁴⁶

cis-Pt(Et)₂(P((CH₂)₁₄)₃P) (cis-7c). A Schlenk flask was charged with *trans*-**2c** (0.3018 g, 0.3291 mmol) and diethyl ether (15 mL). Then a benzene solution of EtLi (0.5 M, 0.200 mL, 0.100 mmol) was added at room temperature with stirring. After 12 h, the mixture was exposed to air. After 1 h, the sample was filtered through celite, which washed with diethyl ether (10-20 mL). The solvent was removed from the filtrate by rotary evaporation. The residue was chromatographed on neutral alumina with hexanes/Et₃N (1:0.005 v/v). The solvent was removed from the product containing fractions by rotary evaporation. The sample was kept at 4 °C for 2 d but did not solidify, affording *cis*-**7c** as a colorless oil (0.2524 g, 0.2791 mmol, 85%).

NMR (CDCl₃, δ /ppm):⁴⁵ ¹H (500 MHz) 1.84-1.75 (br m, 4H, PCH₂), 1.72-1.50 (br m, 12H, PCH₂CH₂), 1.50-1.21 (br m, 68H, remaining CH₂), 1.11-0.81 (br m, 10H, PtCH₂CH₃); ¹³C{¹H} (126 MHz) 31.1 (virtual t,⁴⁷ J_{CP} = 4.2 Hz, CH₂), 30.5 (virtual t,⁴⁷ J_{CP} = 6.7 Hz, CH₂), 28.3 (s, CH₂), 27.5 (s, CH₂), 27.4 (s, CH₂), 26.9 (s, CH₂), 26.8 (s, CH₂), 26.7 (s, CH₂), 26.3 (s, CH₂), 26.1 (s, CH₂), 25.2 (virtual t,⁴⁷ J_{CP} = 2.1 Hz, CH₂), 23.2 (s, CH₂), 23.0 (s, CH₂), 16.4 (t, J_{CP} = 2.1 Hz, PtCH₂CH₃), 14.8 (dd, ²J_{CP(trans)}} = 99.8 Hz, ²J_{CP(cis)}} = 9.1 Hz, PtCH₂CH₃); ³¹P{¹H} (202 MHz) 6.6 (s, ¹J_{Pt(195)}} = 1746 Hz).⁴⁶

trans-Pt(Cl)(Et)(P((CH₂)₁₄)₃P) (trans-8c). Under air, a round-bottom flask was charged with *cis*-**7c** (0.43781 g, 0.4181 mmol), dichloromethane (15 mL), and methanol (1.0 mL). Then CH₃COCl (0.0298 mL, 0.4214 mmol) was added with stirring. After 2 h, the solvent was removed by rotary evaporation. The residue was chromatographed on neutral alumina (5:1:0.02 v/v/v hexanes/dichloromethane/Et₃N). The solvent was removed from the product containing

fractions (TLC monitoring) by rotary evaporation. This gave *trans*-**8c** as a white solid (0.1727 g, 0.1896 mmol, 45%), mp (capillary) 119-131 °C. Anal. Calcd. for C₄₄H₈₉ClP₂Pt: C, 58.03; H, 9.85. Found: C, 58.30; H, 10.02.

NMR (CDCl₃, δ/ppm):⁴⁵ ¹H (500 MHz) 1.89-1.78 (br m, 12H, PCH₂), 1.67-1.57 (br m, 12H, PCH₂PCH₂), 1.48-1.39 (br m, 12H, PCH₂CH₂CH₂), 1.37-1.24 (br m, 48H, remaining CH₂), 1.18-0.98 (br m, 5H, PtCH₂CH₃); ¹³C{¹H} (126 MHz) 30.1 (virtual t,⁴⁷ J_{CP} = 6.7 Hz, CH₂), 28.3 (s, CH₂), 27.4 (s, CH₂), 27.3 (s, CH₂), 26.9 (s, CH₂), 23.5 (s, CH₂), 21.8 (virtual t,⁴⁷ J_{CP} = 15.2 Hz, CH₂), 18.3 (s, PtCH₂CH₃), -9.6 (t, J_{CP} = 5.4 Hz, PtCH₂); ³¹P{¹H} (202 MHz) 10.5 (s, ¹J_{PPt(195)} = 3002 Hz).⁴⁶

Pt(Cl)(Ph)(P((CH₂)₁₄)₃P) (10c). Under air, a round bottom flask was charged with *cis*-Pt(Ph)₂(P((CH₂)₁₄)₃P) (0.0598 g, 0.0598 mmol) and dichloromethane (6 mL). Then a HCl (2.0 M in Et₂O, 0.030 mL, 0.060 mmol) was added at room temperature with stirring. After 1 h (based upon TLC monitoring) another charge of HCl was added (2.0 M in Et₂O, 0.012 mL, 0.024 mmol). After 30 min, the solvent was removed by rotary evaporation to give a white solid, which was chromatographed on neutral alumina (first 5:1 v/v hexanes/dichloromethane, then 20:1 v/v hexanes/ethyl acetate). Two sets of fractions were collected (TLC monitoring). The solvents were removed by rotary evaporation, benzene was added, and the solvent removed by freeze drying. The first set gave *trans*-**10c** (0.0167 g, 0.0174 mmol, 29%)^{4b} as a white powder and the second gave *cis*-**10c** (0.0253 g, 0.0264 mmol, 44%) as a white powder.

did we miss assignments?

Data for *cis*-**10c**: NMR (CDCl₃, δ/ppm):⁴⁵ ¹H (500 MHz) 7.39 (m, *o*-Ph, 2H), 7.05 (t, ¹J_{HH} = 7.48 Hz, 1H, *m*-Ph), 7.04 (t, ¹J_{HH} = 7.48 Hz, 1H, *m*-Ph), 6.89 (t, ¹J_{HH} = 7.29 Hz, 1H, *p*-Ph), 2.54-2.42 (m, 2H), 2.03-1.91 (m, 2H), 1.90-1.73 (m, 4H), 1.72-1.11 (m, 78H); ¹³C{¹H} (126 MHz) 136.1 (s, *o*-Ph), 127.93 (s, *m*-Ph), 127.88 (s, *i*-Ph), 112.8 (s, *p*-Ph), 30.93 (s, CH₂), 30.86 (s, CH₂), 30.77 (s, CH₂), 30.67 (s, CH₂), 30.56 (s, CH₂), 30.43 (s, CH₂), 30.31 (s, CH₂), 27.64 (s, CH₂), 27.43 (s, CH₂), 27.37 (s, CH₂), 27.28 (s, CH₂), 27.14 (s, CH₂), 27.11 (s, CH₂), 26.99 (s, CH₂), 26.94 (s, CH₂), 26.93 (s, CH₂), 26.49 (s, CH₂), 26.39 (s, CH₂), 26.32 (s, CH₂), 26.24 (s,

$\underline{\text{C}}\text{H}_2$), 25.21 (s, $\underline{\text{C}}\text{H}_2$), 25.19 (s, $\underline{\text{C}}\text{H}_2$), 24.84 (s, $\underline{\text{C}}\text{H}_2$), 23.70 (s, $\underline{\text{C}}\text{H}_2$), 23.37 (s, $\underline{\text{C}}\text{H}_2$), 23.24 (s, $\underline{\text{C}}\text{H}_2$), 23.00 (s, $\underline{\text{C}}\text{H}_2$); $^{31}\text{P}\{^1\text{H}\}$ (202 MHz) 5.76 (d, $^2J_{\text{PP}} = 14.0$ Hz, $^1J_{\text{PPt}(195)} = 1671$ Hz, *trans* to Ph),³ 0.18 (d, $^2J_{\text{PP}} = 14.0$ Hz, $^1J_{\text{PPt}(195)} = 4228$ Hz, *cis* to Ph).

Equilibration experiments. The following are representative. **A.** An NMR tube was charged with *cis*-**4c** (0.0134 g, 0.0153 mmol) and $\text{C}_6\text{D}_5\text{Br}$ (0.6 mL). The tube was kept at 110 °C for 7 h and at 140 °C for 6 h. The sample was periodically cooled to room temperature and $^{31}\text{P}\{^1\text{H}\}$ NMR spectra were recorded.

(δ/ppm) 8.94 (s, $^1J_{\text{PPt}} = 2805$ Hz,⁴⁶ >99%). need to discuss

B. An NMR tube was charged with *cis*-**3c** (0.091 g, 0.010 mmol) and $\text{C}_6\text{D}_5\text{Br}$ (0.6 mL). The tube was kept at 110 °C for 7 h. The sample was periodically cooled to room temperature and $^{31}\text{P}\{^1\text{H}\}$ NMR spectra were recorded.

(δ/ppm) 11.15 (s, $^1J_{\text{PPt}} = 2830$ Hz,⁴⁶ >99%). need to discuss

FROM 462: Equilibration Experiments. The following are representative. **A** (Figure 2). An NMR tube was charged with *trans*-**1g** (0.0065 g, 0.0049 mmol) and CH_2Cl_2 (0.7 mL). $^{31}\text{P}\{^1\text{H}\}$ NMR spectra were periodically recorded (after 195 d, δ/ppm): 4.99 (s, $^1J_{\text{PPt}} = 2382$ Hz,⁵¹ *trans*-**1g**, 39%), 0.96 (s, $^1J_{\text{PPt}} = 3515$ Hz,⁵¹ *cis*-**1g**, 61%). **B** (Figure 2). An NMR tube was charged with *trans*-**1g** (0.0064 g, 0.0048 mmol) and toluene (0.7 mL). $^{31}\text{P}\{^1\text{H}\}$ NMR spectra were periodically recorded (after 195 d, δ/ppm): 5.21 (s, $^1J_{\text{PPt}} = 2385$ Hz,⁵¹ *trans*-**1g**, 91%), 1.18 (s, $^1J_{\text{PPt}} = 3518$ Hz,⁵¹ *cis*-**1g**, 9%). The tube was kept at 100 °C for 2 d. The sample was cooled and $^{31}\text{P}\{^1\text{H}\}$ NMR spectra were recorded (δ/ppm): 5.21 (s, $^1J_{\text{PPt}} = 2380$ Hz,⁵¹ *trans*-**1g**, 91%), 1.18 (s, $^1J_{\text{PPt}} = 3513$ Hz,⁵¹ *cis*-**1g**, 9%). **C** (Figure 3). An NMR tube was charged with *trans*-**2'f** (0.0059 g, 0.0050 mmol) and toluene (0.7 mL). $^{31}\text{P}\{^1\text{H}\}$ NMR spectra were periodically recorded (after 86 d, δ/ppm): 4.93 (s, $^1J_{\text{PPt}} = 2374$ Hz,⁵¹ *trans*-**2'f**, 93%), 1.33 (s, $^1J_{\text{PPt}} = 3515$ Hz,⁵¹ *cis*-**2'f**, 7%). The tube was kept at 100 °C for 2 d. The sample was cooled and $^{31}\text{P}\{^1\text{H}\}$ NMR spectra were recorded (δ/ppm): 5.20 (s, $^1J_{\text{PPt}} = 2380$ Hz,⁵¹ *trans*-**2'f**, 93%), 1.17 (s, $^1J_{\text{PPt}}$

= 3513 Hz,⁵¹ *cis-2'f*, 7%). The solvent was removed by rotary evaporation and *o*-C₆H₄Cl₂ (0.7 mL) was added. The tube was kept at 150 °C for 2 d. The sample was cooled and ³¹P{¹H} NMR spectra was recorded (δ/ppm): 5.27 (s, ¹J_{PPt} = 2380 Hz,⁵¹ *trans-2'f*, 93%), 1.33 (s, ¹J_{PPt} = 3514 Hz,⁵¹ *cis-2'f*, 7%).

Crystallography.

A. Methanol was slowly added dropwise to an Et₂O solution of *cis-3c*. After each drop, the mixture was shaken to redissolve the white precipitate formed. When the precipitate persisted, Et₂O was added to regenerate a homogeneous solution, which was kept at 4 °C. After 3 d, colorless crystals were obtained, and data were collected as outlined in Table 1. Cell parameters were obtained from 45 frames using a 1° scan and refined with 102005 reflections. Integrated intensity information for each reflection was obtained by reduction of the data frames with the program APEX3.⁴⁹ Lorentz and polarization corrections were applied. Data were scaled, and absorption correction were applied using the program SADABS.⁵⁰ The space group was determined from systematic reflection conditions and statistical tests. The structure was solved using XT/XS in APEX3.^{49,51} The structure was refined (weighted least squares refinement on *F*²) to convergence.^{51,52} All non-hydrogen atoms were refined with anisotropic thermal parameters. Hydrogen atoms were placed in idealized positions using a riding model. The atoms C29 through C42 and C23 to C24 exhibited elongated thermal ellipsoids and/or nearby residual electron density peaks. These were successfully modeled by disorder between two positions, with occupancy ratios of 0.64:0.36, and 0.81:0.19 respectively. Appropriate restraints and/or constraints were applied to keep the bond distances, angles, and thermal ellipsoids meaningful. The absence of additional symmetry and voids were confirmed using PLATON (ADDSYM).⁵³ **B.** Colorless crystals of *trans-4c* were obtained in a procedure analogous to that for *cis-3c*, but starting from the isomer *cis-4c*. Data were collected and the structure was solved as in **A**. Two pairs of atoms, C11/C1 and C39/C40 exhibited abnormal thermal ellipsoids. These were successfully modeled by disorder between two positions, with occupancy ratios of 0.89:0.11 and 0.88:0.12 respectively. **C.** An

Et₂O solution of *trans*-**6c** was layered with MeOH. After 7 d, data were collected on the yellow blocks as outlined in Table 1. The structure was solved and refined in a manner parallel to that in **A**. The iodide and methyl ligands (I1, C1) were disordered, but this could be modeled and refined to a 86:14 occupancy ratio (I1 and I1a as well as C1 and C1a were constrained to have the same thermal ellipsoids). **D**. Colorless crystals of *trans*-**8c** were obtained in a procedure analogous to that for *cis*-**3c**. Data were collected and the structure was solved in a manner parallel to that in **A**. Three independent molecules were found in the asymmetric unit. For one, the carbon atoms of the methylene chains exhibited elongated thermal ellipsoids (C91-C132), suggesting disorder. This could be modeled between two positions with an occupancy ratio of 0.33-0.67. Appropriate restraints were used to keep bond distances, angles, and thermal ellipsoids meaningful. However, some thermal ellipsoids associated with the modeled positions remained elongated, suggesting further disorder, but no further modeling was attempted.

■ ASSOCIATED CONTENT

● **Supporting Information.** Summaries of ????? and crystallographic data. This material is available free of charge via the Internet at <http://pubs.acs.org>.

The Supporting Information is available free of charge on the ACS Publications website at DOI: 10.1021/acs.(to be determined).

The usual description.

Accession Codes

CCDC 2064494, 2067661, 2067664 and 2070891 contain the supplementary crystallographic data for this paper.

These data can be obtained free of charge via www.ccdc.cam.ac.uk/data_request/cif, or by emailing data_request@ccdc.cam.ac.uk, or by contacting the Cambridge Crystallographic Data Centre, 12 Union Road, Cambridge CB2 1EZ, UK; fax: +44 1123 336033.

■ AUTHOR INFORMATION

Corresponding Author

E-mail: gladysz@mail.chem.tamu.edu

‡Deceased 28 October 2020.

ORCID ●

Yun Zhu: 0000-0003-0123-6827

Andreas Ehnbohm: 0000-0002-7044-1712

Tobias Fiedler: 0000-0001-7169-305X

Michael B. Hall: 0000-0003-3263-3219

John A. Gladysz: 0000-0002-7012-4872

Notes

The authors declare no competing financial interest.

■ ACKNOWLEDGMENTS

The authors thank the US National Science Foundation (JAG: CHE-1566601, CHE-1900549; MBH: CHE-1664866) for support.

■ REFERENCES

(1) Kottas, G. S.; Clarke, L. I.; Horinek, D.; Michl, J. Artificial Molecular Rotors. *Chem. Rev.* **2005**, *105*, 1281-1376.

(2) dummy

(3) Ehnbohm, A.; Gladysz, J. A. Gyroscopes and the Chemical Literature, 2002-2020: Approaches to a Nascent Family of Molecular Devices. *Chem. Rev.* **2021**, *121*, in press.

(4) (a) Nawara-Hultsch, A. J.; Stollenz, M.; Barbasiewicz, M.; Szafert, S.; Lis, T.; Hampel, F.; Bhuvanesh, N.; Gladysz, J. A. Gyroscope-Like Molecules Consisting of PdX₂/PtX₂ Rotators within Three-Spoke Dibrigehead Diphosphine Stators: Syntheses, Substitution Reactions, Structures, and Dynamic Properties. *Chem. Eur. J.* **2014**, *20*, 4617-4637. (b) Taher, D.; Nawara-Hultsch, A. J.; Bhuvanesh, N.; Hampel, F.; Gladysz, J. A. Mono- and Disubstitution Reactions of Gyroscope Like Complexes Derived from Cl-Pt-Cl Rotators within Cage Like Dibrigehead Diphosphine Ligands. *J. Organomet. Chem.* **2016**, *821*, 136-141. (c) Kharel, S.; Joshi, H.; Bhuvanesh, N.; Gladysz, J. A. Syntheses, Structures, and Thermal Properties of Gyroscope-like Complexes Consisting of PtCl₂ Rotators Encased in Macrocyclic Dibrigehead Diphosphines P((CH₂)_n)₃P with Extended Methylene Chains (*n* = 20/22/30) and Isomers Thereof. *Organometallics*, **2018**, *37*, 2991-3000.

(5) (a) Wang, L.; Hampel, F.; Gladysz, J. A. 'Giant' Gyroscope-Like Molecules Consisting of Dipolar Cl-Rh-CO Rotators Encased in Three-Spoke Stators That Define 25-27-Membered Macrocycles. *Angew. Chem. Int. Ed.* **2006**, *45*, 4372-4375; 'Gyroskop-Giganten': Dipolare Cl-Rh-CO-Rotatoren, umgeben von Statoren aus drei Speichen 25- bis 27-gliedriger Makrocyclen. *Angew. Chem.* **2006**, *118*, 4479-4482. (b) Wang, L.; Shima, T.; Hampel, F.; Gladysz, J. A. Gyroscope-like molecules consisting of three-spoke stators that enclose "switchable" neutral dipolar rhodium rotators; reversible cycling between faster and slower rotating Rh(CO)I and Rh(CO)₂I species. *Chem. Commun.* **2006**, 4075-4077. (c) Estrada, A. L.; Jia, T.; Bhuvanesh, N.; Blümel, J.; Gladysz, J. A. Substitution and Catalytic Chemistry of Gyroscope-Like Complexes Derived from Cl-Rh-CO Rotators and Triply *trans* Spanning

Di(trialkylphosphine) Ligands. *Eur. J. Inorg. Chem.* **2015**, *2015*, 5318-5321.

(6) (a) Lang, G. M.; Shima, T.; Wang, L.; Cluff, K. J.; Skopek, K.; Hampel, F.; Blümel, J.; Gladysz, J. A. Gyroscope-Like Complexes Based on Dibridgehead Diphosphine Cages That Are Accessed by Three-Fold Intramolecular Ring Closing Metatheses and Encase Fe(CO)₃, Fe(CO)₂(NO)⁺, and Fe(CO)₃(H)⁺ Rotators. *J. Am. Chem. Soc.* **2016**, *138*, 7649-7663. (b) Lang, G. M.; Bhuvanesh, N.; Reibenspies, J. H.; Gladysz, J. A. Syntheses, Reactivity, Structures, and Dynamic Properties of Gyroscope-like Iron Carbonyl Complexes Based on Dibridgehead Diarsine Cages. *Organometallics*, **2016**, *35*, 2873-2889. (c) Lang, G. M.; Skaper, D.; Hampel, F.; Gladysz, J. A. Synthesis, reactivity, structures, and dynamic properties of gyroscope like iron complexes with dibridgehead diphosphine cages: pre- vs. post-metathesis substitutions as routes to adducts with neutral dipolar Fe(CO)(NO)(X) rotors. *Dalton Trans.* **2016**, *45*, 16190-16204.

(7) (a) Fiedler, T.; Bhuvanesh, N.; Hampel, F.; Reibenspies, J. H.; Gladysz, J. A. Gyroscope like molecules consisting of trigonal or square planar osmium rotators within three-spoked dibridgehead diphosphine stators: syntheses, substitution reactions, structures, and dynamic properties. *Dalton Trans.* **2016**, *45*, 7131-7147. (b) Hess, G. D.; Fiedler, T.; Hampel, F.; Gladysz, J. A. Octahedral Gyroscope-like Molecules Consisting of Rhenium Rotators within Cage-like Dibridgehead Diphosphine Stators: Syntheses, Substitution Reactions, Structures, and Dynamic Properties. *Inorg. Chem.* **2017**, *56*, 7454-7469.

(8) Joshi, H.; Kharel, S.; Ehnbohm, A.; Skopek, K.; Hess, G. D.; Fiedler, T.; Hampel, F.; Bhuvanesh, N.; Gladysz, J. A. Three-Fold Intramolecular Ring Closing Alkene Metatheses of Square Planar Complexes with *cis* Phosphorus Donor Ligands P(X(CH₂)_mCH=CH₂)₃ (X = -, *m* = 5-10; X = O, *m* = 3-5): Syntheses, Structures, and Thermal Properties of Macrocyclic Dibridgehead Diphosphorus Complexes. *J. Am. Chem. Soc.* **2018**, *140*, 8463-8478.

(9) Taher, D.; Nawara-Hultsch, A. J.; Bhuvanesh, N.; Hampel, F.; Gladysz, J. A. Mono- and disubstitution reactions of gyroscope like complexes derived from Cl-Pt-Cl rotators within cage like dibridgehead diphosphine ligands. *J. Organomet. Chem.* **2016**, *821*, 136-141.

(10) dummy

(11) dummy

(12) Grim, S. O.; Keiter, R. L.; McFarlane, W. A phosphorus-31 nuclear magnetic resonance study of tertiary phosphine complexes of platinum(II). *Inorg. Chem.* **1967**, *6*, 1133-1137.

(13) Nawara-Hultsch, A. J.; Skopek, K.; Shima, T.; Barbasiewicz, M.; Hess, G. D.; Skaper, D.; Gladysz, J. A. Syntheses and Palladium, Platinum, and Borane Adducts of Symmetrical Trialkylphosphines with Three Terminal Vinyl Groups, $P((CH_2)_mCH=CH_2)_3$. *Z. Naturforsch.* **2010**, *65b*, 414-424.

(16) (a) Bondi, A. van der Waals Volumes and Radii. *J. Phys. Chem.* **1964**, *68*, 441-451.

(b) Mantina, M.; Chamberlin, A. C.; Valero, R.; Cramer, C. J.; Truhlar, D. G. Consistent van der Waals Radii for the Whole Main Group. *J. Phys. Chem. A* **2009**, *113*, 5806-5812.

(45) The 1H and ^{13}C NMR assignments were made by analogy to those in reference [4](#), which were established by 2D NMR experiments.

(46) This coupling represents a satellite (d, $^{195}Pt = 33.8\%$) and is not reflected in the peak multiplicity given.

(47) Hersh, W. H. False AA'X Spin-Spin Coupling Systems in ^{13}C NMR: Examples Involving Phosphorus and a 20-Year-Old Mystery in Off-Resonance Decoupling. *J. Chem. Educ.* **1997**, *74*, 1485-1488. The J values represent the distance between adjacent peaks in the apparent triplet.

(48) m/z (relative intensity, %), MALDI+; the most intense peak of isotope envelope is given.

(49) *APEX3*, Bruker AXS Inc., Madison, WI, USA, 2012.

(50) Sheldrick, G. M. *SADABS*, Bruker AXS Inc., Madison, WI, USA, 2001.

(51) (a) Sheldrick, G. M. A short history of *SHELX*. *Acta Cryst.* **2008**, *A64*, 112-122. (b) Sheldrick, G. M. SHELXT – Integrated space-group and crystal-structure determination. *Acta*

Cryst. **2015**, *A71*, 3-8.

(52) Dolomanov, O. V.; Bourhis, L. J.; Gildea, R. J. Howard, J. A. K.; Puschmann, H. OLEX2: A Complete Structure Solution, Refinement and Analysis Program. *J. Appl. Crystallogr.* **2009**, *42*, 339-341.

(53) Spek, A. L. Single-crystal structure validation with the program *PLATON*. *J. Appl. Crystallogr.* **2003**, *36*, 7-13.

Table 1. Summary of crystallographic data.

	<i>cis-3c</i>	<i>trans-4c</i>	<i>trans-6c</i>	PtMeI
empirical formula	C ₄₄ H ₉₀ P ₂ Pt	C ₄₃ H ₈₇ ClP ₂ Pt	C ₄₄ H ₈₉ ClP ₂ Pt	C ₄₃ H ₈₇ IP ₂ Pt
formula weight	876.18	896.60	910.63	988.05
Temperature [K]	110(2)	110(2)	110(2)	110(2)
diffractometer	Quest	Quest	APEX II	APEX II
wavelength [Å]	0.71073	0.71073	0.71073	0.71073
crystal system	monoclinic	monoclinic	monoclinic	orthorhombic
space group	P 1 2 ₁ /c 1	P 1 2 ₁ /n 1	P 1 2 ₁ /c 1	<i>Pbca</i>
unit cell dimensions:				
<i>a</i> [Å]	10.3514(4)	16.2658(9)	38.540(7)	20.481(6)
<i>b</i> [Å]	15.4895(6)	13.6513(8)	14.255(3)	13.685(4)
<i>c</i> [Å]	28.4607(12)	19.9653(11)	25.681(4)	33.232(10)
α [°]	90	90	90	90
β [°]	95.7670(10)	90.090(2)	91.995(2)	90
γ [°]	90	90	90	90
<i>V</i> [Å ³]	4540.2(3)	4432.7(4)	14100(4)	9314(5)
<i>Z</i>	4	4	12	8
ρ _{calc} [Mg/m ⁻³]	1.282	1.344	1.287	1.409
μ [mm ⁻¹]	3.188	3.325	3.137	3.770
<i>F</i> (000)	1848	1880	5736	4048
crystal size [mm ³]	0.441 × 0.207 × 0.182	0.493 × 0.475 × 0.292	0.10 × 0.10 × 0.10	0.56 × 0.16 × 0.12
Θ limit [°]	1.949 to 24.999	1.948 to 27.496	1.66 to 27.50	2.336 to 27.497
index range (<i>h, k, l</i>)	-12, 12; -18, 18; -33, 33	-21, 21; -17, 17; -25, 25	-50, 50; -18, 18; -33, 33	-26, 26; -17, 17; -43, 43
reflections collected	102005	173120	154056	97076
independent reflections	7997	10146	32379	10629
<i>R</i> (int)	0.0451	0.0537	0.0930	0.0463
completeness to Θ	99.9	99.8	99.9	99.6
max. and min. transmission	0.4291 and 0.1274	0.2616 and 0.0906	0.7457 and 0.4356	0.7456 and 0.4890
data/restraints/parameters	7997/801/566	10146/123/459	32379/1956/1676	10629/3/426
goodness-of-fit on <i>F</i> ²	1.073	1.056	1.056	1.076
<i>R</i> indices (final) [<i>I</i> > 2σ(<i>I</i>)]				
<i>R</i> ₁	0.0331	0.0183	0.0585	0.0353
<i>wR</i> ₁	0.0695	0.0387	0.1194	0.0837
<i>R</i> indices (all data)				
<i>R</i> ₂	0.0378	0.0226	0.0934	0.0493
<i>wR</i> ₂	0.0732	0.402	0.1364	0.0918
largest diff. peak and hole [eÅ ⁻³]	2.107 and -2.309	0.683 and -0.795	1.927 and -1.925	2.037 and -1.132

Table 2. Key distances involving parachute or gyroscope like complexes.

	<i>cis-3c</i> ^a	<i>trans-4c</i> ^a	<i>trans-6c</i> ^a	<i>trans-8c(1)</i> ^b	<i>trans-8c(2)</i> ^b	<i>trans-8c(3)</i> ^b
Pt–P	2.2844(11) 2.2818(11)	2.2810(5) 2.2920(5)	2.2946(12) 2.3032(13)	2.2887(16) 2.3089(16)	2.2848(19) 2.3037(19)	2.284(2) 2.285(2)
P to P	3.602(2)	4.5715(6)	4.594(2)	4.587(2)	4.587(3)	4.560(3)
Pt–L ^c	2.105(4) 2.106(5)	2.074(7)	2.179(5)	2.102(6)/3. 024 ^d	2.093(8)/3. 091 ^d	2.104(8)/3. 006 ^d
Pt–L _{rotor} ^c	3.81	3.77	3.88	4.72	4.79	4.71
Pt–X ^e	–	2.4020(6)	2.6864(8)	2.4052(16)	2.401(2)	2.408(2)
Pt–X _{rotor} ^f	–	4.15	4.67	4.16	4.15	4.16

^aValues for the dominant X–Pt–Y rotamer orientation. ^bValues for the three independent molecules in the unit cell. ^cL = Me, Et. ^dDistances from platinum to key atoms of L (L = Me, Et) or X (O₂CO). The first value is for the atoms directly bound to platinum, and the second is for the most remote carbon or oxygen atom. ^eX = Cl, Br, I. ^fThe Pt–X distance plus the van der Waals radius of X (Cl, 1.75 Å; Br, 1.85 Å; I, 1.98 Å; O, 1.50 Å).

NEED TO DRAFT DISCUSSION BEFORE TABLE CAN BE FINALIZED

TABLE OF CONTENTS GRAPHIC

